MUC-NOTE-COOL_THEORY-317

Heating in the Study 2a absorber window

R.C. Fernow
Brookhaven National Laboratory

13 May 2005

We examine the temperature distribution in the 3-layer Be-LiH-Be absorber windows used for Study 2a. Heat from dE/dx losses is deposited in all the layers. An additional contribution from rf heating is deposited in the Be layer facing the rf cavity. We determine the maximum temperature reached in each layer using a 1-dimensional solution of the heat conduction equation. Time-varying material properties and radiation losses are included in the analysis. A new design is presented where the maximum temperature reached in the LiH is 580 K, while the maximum temperature in the Be layer facing the rf cavity is 445 K.

1. Introduction

The cooling channel for the neutrino factory in Study 2a (ST2a) made use of novel absorbers that also served as the windows for the rf cavities [1]. In ST2a the absorbers consisted of a 1 cm thick layer of LiH with 25 μm thick layers of beryllium on both sides. The purpose of the Be was to protect the LiH from the environment and to provide a metallic boundary for the end of the rf cavity. All the layers are heated from dE/dx losses from the muon beam. In addition, the Be layer facing the rf cavity must also absorb the rf cavity wall-losses in a skin depth along the cavity.

The absorber design is shown schematically in Fig. 1.

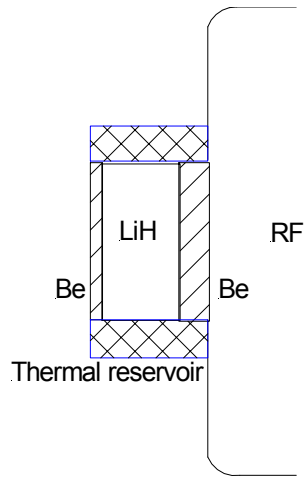

Figure 1. The ST2a cooling channel absorber/rf window design. (not to scale)

In this report we will allow the thicknesses of the two Be layers to be different, since the power deposition is different for the two layers. The window radius is 25 cm and the radius of the rf cavity is 58 cm.

It is important to determine the temperature distributions in the layers, the time for the layers to reach thermal equilibrium, and the maximum temperature that is reached in each layer. We solve the problem in this report by breaking each layer into a series of annular rings and solving the diffusion equation numerically. A 1-dimensional analysis is used here. This means that heat conduction can only take place radially. A thermal reservoir is located outside the outer radius of the window. No axial heat conduction is allowed, so the analysis of each window layer is independent of the others.

2. Power distributions

There are two sources of incident power P. First, there is dE/dx heating caused by the muon beam passing through the absorber. For a 1 MW beam we assume 10^{14} protons/pulse with a 2.5 Hz pulse repetition rate, 2 charges and 0.45 μ/p at the entrance to the cooling channel. This gives an incident muon flux of 2.26 10^{14} μ/s. The beam power deposited per unit length in the material is then

$$\frac{dP_b}{dz}\left[\frac{W}{cm}\right] = 36\frac{dE}{dz}\left[\frac{MeV}{cm}\right]$$

To get the total deposited beam power P_{b0} we must multiply by the thickness of the layer. For example, the total 1 MW beam power deposited in the 1 cm thick layer of LiH is 58 W.

We assume the beam power has a radially symmetric Gaussian distribution

$$\frac{dP_b}{dA} = \frac{P_{b0}}{2\pi\sigma^2} e^{-\frac{1}{2}\left(\frac{r}{\sigma}\right)^2}$$

We use a standard deviation σ of 5 cm. The incident power deposited on the rings for the 1 cm layer of LiH is shown in Fig. 2.

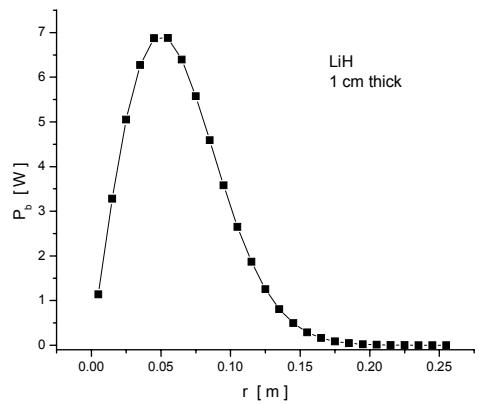

Figure 2. Distribution of incident beam power on the LiH annular rings.

Although the gaussian distribution is centered on the axis, the ring area grows with r and this causes the deposited beam power to peak at r~5 cm.

The second source of heating is due to the rf fields in the 201 MHz cavity. This deposits power in a skin depth of the Be layer that faces the cavity. The skin depth is given by

$$\delta = \sqrt{\frac{\eta}{\pi\mu_o f}}$$

where η is the electrical resistivity, μ_o is the permeability of free space and *f* is the rf frequency. Using the room temperature resistivity of beryllium, we find the skin depth is ~9 μm.

The rf surface heating is given by

$$\frac{dP_{rf}}{dA} = f_d \frac{E^2}{Z_o} \frac{\pi}{2} \frac{\delta}{\lambda} J_1^2\left(x_{01} \frac{r}{r_c}\right)$$

where f_d is the pulse duty factor, *E* is the electric field strength, $Z_o = 377\ \Omega$ is the impedance of free space, λ is the rf wavelength, J_1 is a Bessel function, $x_{01} = 2.405$ is the first zero of the J_0 Bessel function, and r_c is the radius of the cavity. For the present case we have $f_d = 1.9\ 10^{-3}$, $E = 15.25$ MV/m, $\lambda = 1.49$ m, and $r_c = 0.58$ m. This function

reaches its maximum at a radius of 45 cm, which lies beyond the 25 cm radius of the window. Thus the local rf heating is 0 on the beam axis and increases steadily up to the window radius. The power distribution in the 1 cm radial rings is shown in Fig. 3.

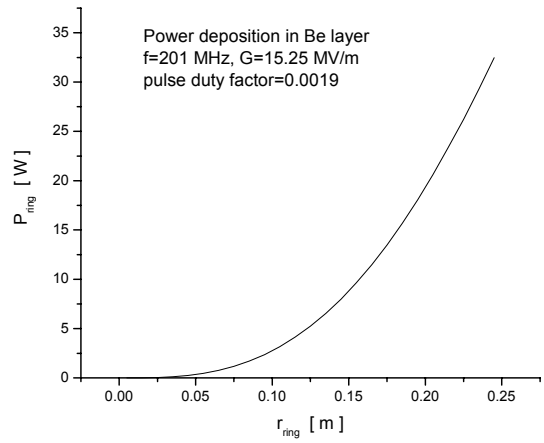

Figure 3. Distribution of incident rf power on the Be annular rings.

We can find the total power deposited in the layer by integrating the area up to the radius of the window r_w

$$P_{rf} = \frac{\pi^2}{2} f_d \frac{\delta}{\lambda} \frac{E^2 r_w^2}{Z_o} \left[J_1^2(\alpha) - J_0(\alpha) J_2(\alpha) \right]$$

where the argument of the Bessel function $\alpha = x_{01}\, r_w / r_c$. For the 25 cm radius window considered here, the total rf power is 220 W.

In addition thermal radiation from a hot surface represents a power sink given by

$$P_{rad} = \varepsilon A \sigma_{SB} \left(T^4 - T_R^4 \right)$$

where ε is the emissivity of the surface, A is the surface area, $\sigma_{SB} = 5.67\ 10^{-8}$ W/m^2/K^4 is the Stefan-Boltzmann constant, and T_{RES} is the temperature of the thermal reservoir. We use a room temperature (300 K) reservoir in this report.

3. Heat conduction equation

The approach of a temperature distribution to equilibrium is an example of the diffusion equation [2]. Let us break each layer into a series of annular rings. We assume that a thermal reservoir fixed at 300 K exists along the outer edge of the window. Including a constant source term the diffusion equation for heat conduction is

$$\frac{\partial T}{\partial t} - \frac{\kappa(T)}{\rho C(T)} \nabla^2 T = \frac{P}{mC(T)}$$

The temperature T is a function of the radius r and time t. The specific heat C, thermal conductivity κ, and density ρ are functions of the temperature. Values for some of these quantities at room temperature are given in Table 1.

Table 1. Material properties at room temperature

		LiH	Be
ρ	g / cm^3	0.75	1.848
C	J / K / kg	3670	1825
κ	W / m / K	8	201
η	μΩ - cm		5.89
T_{melt}	K	962	1551

The incident power is P and the mass of an annular ring is m. We assume the problem has azimuthal symmetry. The 1-D Laplacian in cylindrical coordinates is then

$$\nabla^2 = \frac{\partial^2}{\partial r^2} + \frac{1}{r}\frac{\partial}{\partial r}$$

The diffusion coefficient is

$$D = \frac{\kappa}{\rho C}$$

and the source term is

$$S = \frac{P}{m\,C}$$

We solve the problem numerically using finite differences. We break the 25 cm window into 25 radial rings, each with a radial width of 1 cm. Let j refer to spatial variations and n refer to time steps. Then we have

$$\frac{T_j^{n+1} - T_j^n}{\Delta t} - D\left[\frac{T_{j+1}^{n+1} - 2T_j^{n+1} + T_{j-1}^{n+1}}{(\Delta r)^2} + \frac{1}{r}\left(\frac{T_{j+1}^{n+1} - T_{j-1}^{n+1}}{2\Delta r}\right)\right] = S_j^n$$

The problem can be solved by combining all the terms that depend on the new time step (n+1) on the left side of the equation and putting all the other terms on the right side [3]. Then one has a matrix equation that can be solved for the temperature values at the new time step.

The results of the 1-D calculations with <u>constant</u>, room temperature material properties are summarized in Table 2. The axial thickness of the layer is denoted d, the maximum temperature is T_{max} and the time for the temperature distribution to come to equilibrium is t_{eq}.

Table 2. Results of 1-D calculation with constant material properties.

	d	T_{max}	t_{eq}
		K	min
LiH	1 cm	479	399
Be	25 μm	2498	26
Be	100 μm	860	22

The maximum temperature occurs on the beam axis. The maximum temperature in the LiH layer is well below the melting temperature. However, the maximum temperature in the 25 μm layer of Be used in ST2a is far above the melting temperature of Be. We can increase the thickness of the Be layer on the side facing the rf cavity up to ~100 μm to bring the maximum temperature down to a more reasonable level.

4. Window heating with temperature-dependent material properties

We now consider the effect of the temperature dependence of the material properties. This is shown in Fig. 4 for LiH [4].

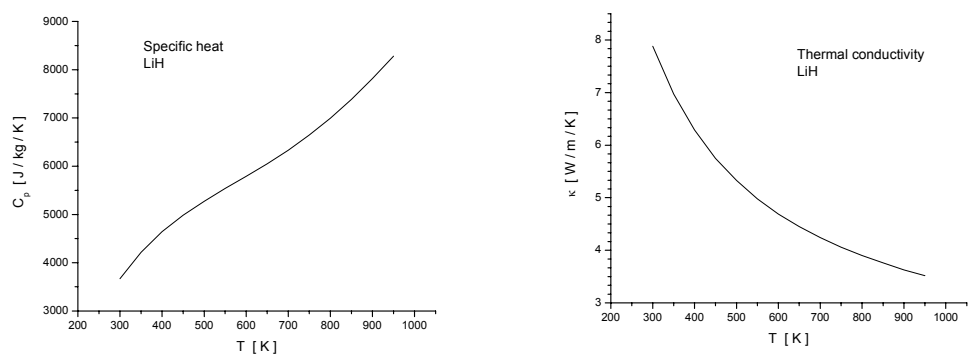

Figure 4. Specific heat (left) and thermal conductivity (right) of LiH as a function of temperature.

As the temperature increases the specific heat increases steadily, while the thermal conductivity falls by about a factor of 2.

The same quantities are shown for Be [5,6] in Fig. 5.

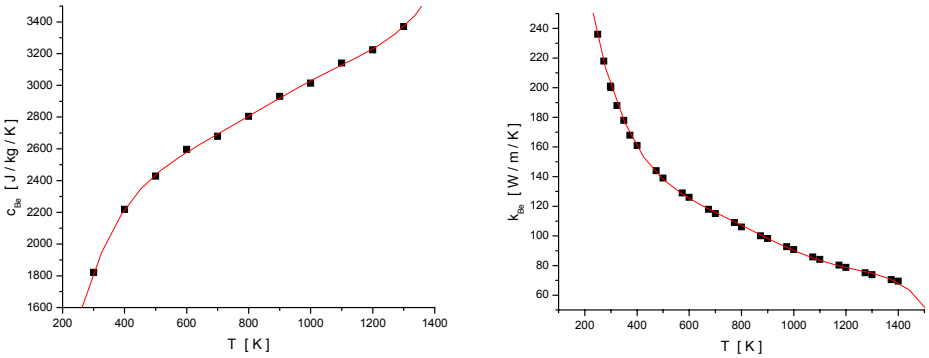

Figure 5. Specific heat (left) and thermal conductivity (right) of Be as a function of temperature.

As the temperature increases the specific heat increases steadily, while the thermal conductivity falls by about a factor of 3. The fall-off of the thermal conductivity of both materials with increasing temperature is particularly significant since it will allow the temperature to build up to higher values than those estimated in the previous section. The electrical resistivity of Be [5] also increases with temperature, as shown in Fig. 6.

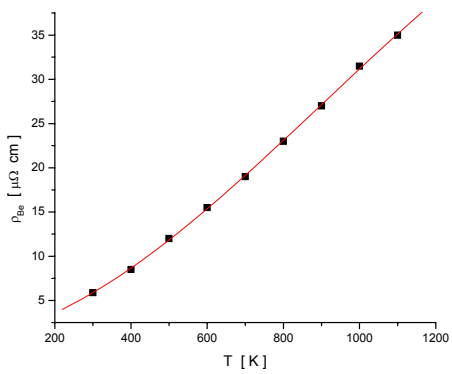

Figure 6. Electrical resistivity of Be as a function of temperature.

This causes a change of up to a factor of ~2 in the skin depth.

We now examine the solution of the 1-D diffusion equation with temperature-dependent coefficients. The spatial and temporal temperature distributions for LiH are shown in Fig. 7.

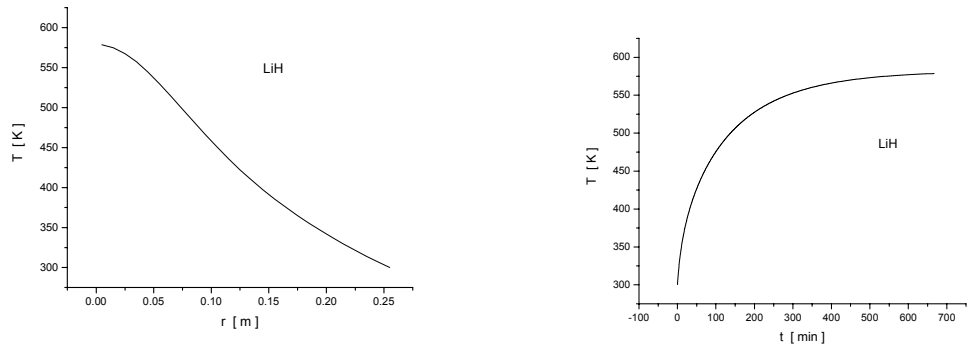

Figure 7. Radial (left) and time dependence (right) for the 1 cm LiH layer.

The variable material properties cause the maximum temperature in the LiH to reach 580 K, which is ~100 K higher than the constant case. The time to reach equilibrium also increases by ~200 minutes to around 600 minutes.

The maximum temperature of the Be layer facing the rf cavity is shown in Fig. 8 as a function of the layer thickness.

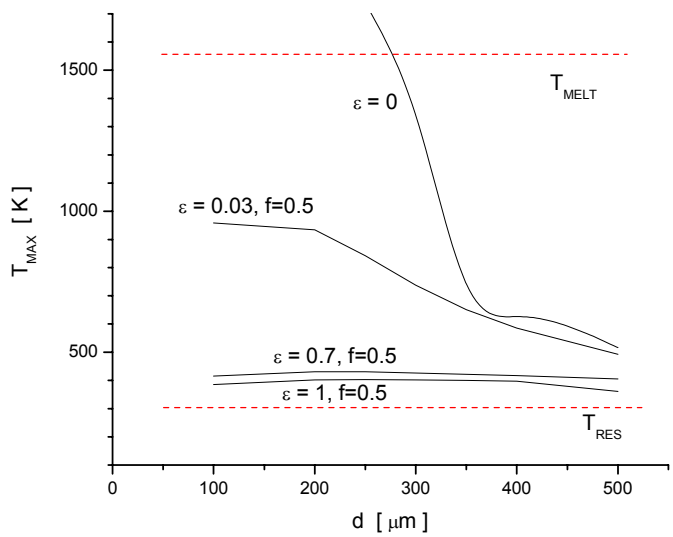

Figure 8. Maximum temperature of the hot Be layer as a function of layer thickness.

The thermal radiation from the hot surface plays a crucial role here. Without radiation ($\varepsilon = 0$) layers thinner than ~275 μm would melt. Therefore we assume the cavity walls are maintained at 300 K. (The total power losses in the walls of a real 201 MHz cavity are estimated to be ~9.3 kW [7]. Cooling the cavity walls to 77 K has been discussed in the past, which would be even better). The rf cavity contains two parallel windows. Thermal radiation from a given window cannot be absorbed on the other window, which by

symmetry must be at the same temperature. Thus in order for thermal radiation to be effective, it must fall on the cavity wall outside the opposite window[1]. This effect introduces a factor *f* that must multiply the emissivity (see Appendix A). For a 25 cm window we find that $f = 0.50$. The temperature for a perfectly emitting surface ($\varepsilon = 1$) would reach a maximum temperature of 403 K. A web search [8] for the emissivity of beryllium metal showed that a typical value was $\varepsilon \sim 0.03$. For a thickness of 300 μm the maximum temperature was 738 K. However, the Be window will be coated with a very thin layer of titanium nitride to reduce secondary electron emission.[2] A web search [9] for the emissivity of TiN showed that $\varepsilon \sim 0.7$. The temperature distribution in this case was very similar to the $\varepsilon = 1$ results. The temperature distributions for a 300 μm Be layer with a TiN coating is shown in Fig. 9.

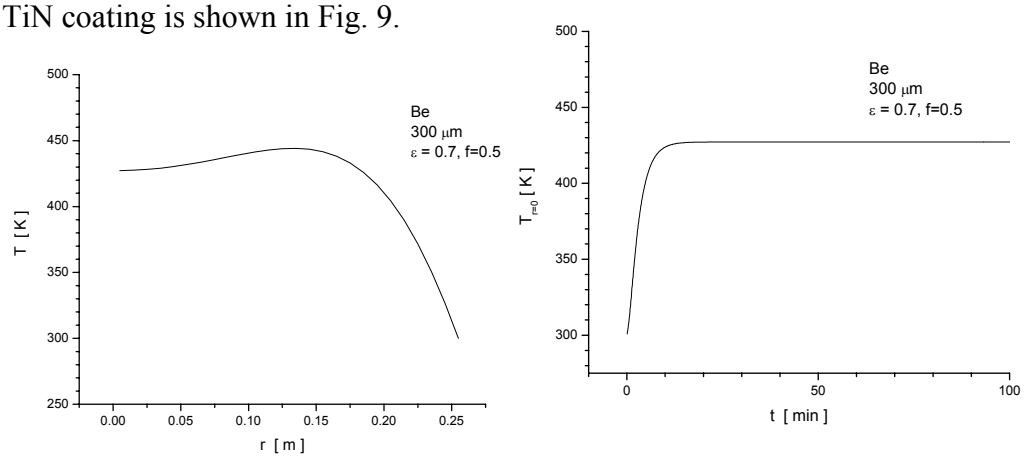

Figure 9. Radial (left) and time dependence (right) for the 300 μm Be layer facing the rf cavity. The emissivity of TiN is used for the calculation.

The maximum temperature of 445 K occurs at a radius of 15 cm. The temperature reaches equilibrium in about 15 minutes. The temperature distribution for the 25 μm Be layer <u>not</u> facing the rf cavity is shown in Fig. 10.

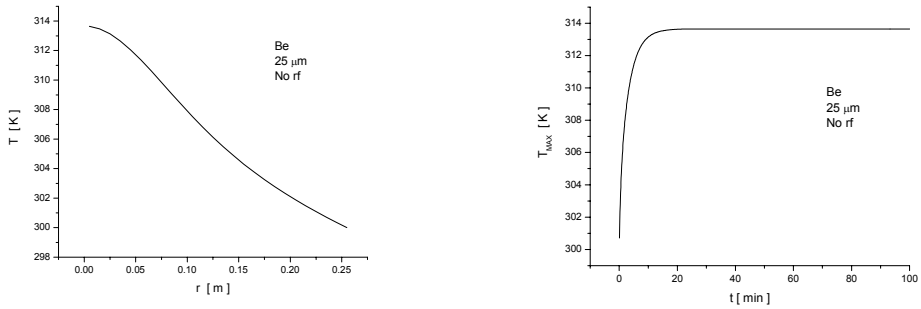

Figure 10. Radial (left) and time dependence (right) for the 25 μm Be layer not facing the rf cavity.

There is no problem with heating in this layer.

---

[1] Thanks to Scott Berg for pointing this out.
[2] And thanks to Jim Norem for reminding us about this.

5. Ionization cooling with new window design

We have been lead to a modified window design consisting of a 25 μm Be outer layer, a 1 cm LiH layer and a 300 μm Be layer facing the rf cavity. The question now is whether the extra beryllium degrades the ionization cooling in the channel. The number of muons per incident proton in the Study 2a accelerator acceptance is shown in Fig. 11.

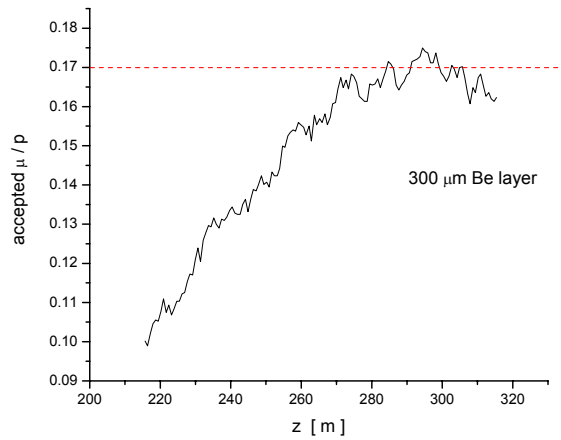

Figure 11. Accepted muons per proton in the modified cooling channel.

We see that the accepted number of muons still exceeds the require value of 0.17 for the nominal 80 m cooling channel (ending at 295 m in the figure).

6. 4 MW beam power

It is also important to consider whether this absorber design could also be used with an upgraded 4 MW proton driver. The results are shown in Table 3.

Table 3. Results of 4 MW beam power calculations.

	d	T_{max}	t_{eq}
		K	min
LiH	1 cm	4080	2660
Be	25 μm	360	24
Be	300 μm	455	13

The Be layers can handle the extra beam power, but the LiH clearly cannot.

7. Conclusions

On the basis of this 1-D analysis a 3-layer absorber design with a ~300 μm thick Be layer on the side facing the rf cavity still appears feasible for 1 MW beam power. However, longitudinal heat conduction could still have a significant effect on these results, so a 2-D thermal analysis is needed next. Eventually a full analysis of the absorber design must be

done with a finite elements code, such as ANSYS, and the design must be validated with a program of experimental R&D. This will be required to examine thermally induced stresses that could lead to delamination or buckling. The simple absorber design discussed here will clearly not work for 4 MW beam power. Fortunately, a number of alternative window designs have been suggested, such as finer grained Be-LiH sandwiches [10], convective gas layers[3], and graded-thickness curved windows. Detailed examination of these designs would also require the use of a code like ANSYS.

Appendix A. Parallel-window radiation cooling efficiency

We consider here the derivation of the effective cooling efficiency factor. Figure A1 shows the two parallel windows in the pillbox rf cavity. Let the radius of the window be *b* and the length of the cavity be *L*.

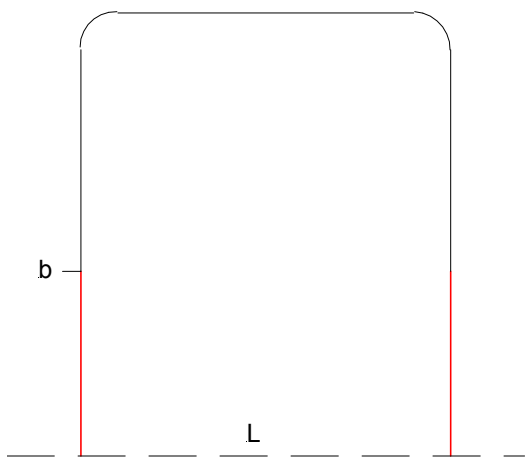

Figure A1. Scale drawing of the upper half of the pillbox rf cavity. (b=25 cm, L=50 cm)

Consider the radiation cooling of the left circular window. We assume the radiation leaves a surface element at radius *r* in a cone of angle θ. We assume the probability of emission at the angle θ is proportional to cos θ .When the radiation cone reaches the opposite surface it is spread out over a circle of radius a = L tan θ. The portion of the projected cone that intercepts the opposite window cannot lead to net cooling since both windows must be at the same temperature. Define the effective cooling efficiency as

$$f(b,L) = 1 - \frac{P_{win}}{P_{tot}}$$

where P_{win} is the radiated power that intercepts the opposite window and P_{tot} is the maximum possible radiated power. Let dP/dA be the average power emission per unit area.

[3] Early examination of this approach looks promising. R. Palmer, private communications, 13 May 2005.

Then

$$P_{tot} = \frac{dP}{dA}\pi b^2$$

is the total possible radiated power. The power hitting the opposite window is

$$P_{win} = 2\pi \frac{dP}{dA}\int_0^b \int_0^{\frac{\pi}{2}} \cos\theta \; g(r,\theta) \; d\theta \; r \; dr$$

where g(r, θ) is the fraction of the radiation cone emitted at the angle θ from the surface element at radius *r* that intercepts the opposite window. There are three cases for determining *g*.

(I) a < b-r
$g = 1$

(II) a > b+r
$g = b^2 / a^2$

(III) b-r < a < b+r

$$g = \frac{2}{\pi a^2}\left[\int_{r-a}^{x_2} \sqrt{a^2 - (x-r)^2}\, dx + \int_{x_2}^{b} \sqrt{b^2 - x^2}\, dx\right]$$

The parameter x_2 is given by

$$x_2 = \frac{b^2 - a^2 + r^2}{2r}$$

The dependence of the cooling efficiency *f* on the window radius *b* is shown in Fig. A2.

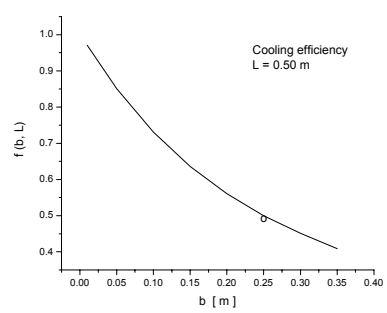

Figure A2. Radiation cooling efficiency factor as a function of the window radius.

For *b* = 0.25 m and *L* = 0.50 m, the factor *f* is 0.50.

Acknowledgements

We would like to thank Scott Berg, Juan Gallardo, Dan Kaplan, Jim Norem and Bob Palmer for useful discussions.

References

[1] C. Albright et al., Neutrino factory and beta beam experiments and development, in APS Joint Study on the Future of Neutrino Physics, BNL-72369 (2004); Muon Collaboration technical note MUC-NOTE-COOL_THEORY-312.
[2] W. Kaplan, Advanced Calculus, Addison-Wesley, Reading, MA, 1952, p. 295.
[3] W. Press et al., Numerical Recipes in Fortran, 2nd ed., Cambridge University Press, Cambride, UK, 1992, p. 838.
[4] R. Terry, Lithium hydride debris shields for plasma radiation sources, report NRL/MR/6720-96-7868 (1996).
[5] A. Goldsmith et al., Handbook of thermophysical properties of solid materials, Vol. 1: Elements, Macmillan, New York, 1961.
[6] Thermal conductivity of the elements, J. Phys. Chem. Ref. Data, Vol. 3, Suppl.1, 1974.
[7] R. Rimmer et al., Closed cell 201.25 MHz rf structuresfor a muon cooling channel, Proc. PAC 2001, p. 927.
[8] Epner Technology Inc., Laser Gold Emissivity Data, http://www.epner.com/laser_emissivity.ssi
[9] Coating technical product data, ZYP Coatings, Inc., Oak Ridge, TN.
[10] J. Cobb & H. Witte, Estimates of the temperatures of LiH absorbers, 22 June 2004.